

Degradation of chlorotriazine pesticides by sulfate radical anions and influence of organic matter

Prepared on July, 2014

Holger Lutze^{1,2}, Stefanie Bircher¹, Insa Rapp¹, Nils Kerlin¹, Rani Bakkour¹, Melanie Geisler¹,
Clemens von Sonntag^{1,3} and Torsten C. Schmidt^{1,2,4}*

(1) University Duisburg-Essen, Instrumental Analytical Chemistry Universitätsstr. 5 D-45141 Essen, Germany,

(2) IWW Water Centre, Moritzstr. 26, D-45476 Mülheim an der Ruhr, Germany, (3) Max-Planck-Institut für

Chemische Energiekonversion, Stiftstrasse 34-36, P.O. Box 101365, D-45470 Mülheim an der Ruhr, Germany

(4) Centre for Water and Environmental Research, Universitätsstraße 2, D-45117 Essen

e-mail: holger.lutze@uni-due.de

Ten pages of Supporting Information, including 6 narratives and 4 figures:

Text S1 Competition kinetics

Text S2 Calculation of fractions reacting with an oxidant

Text S3 Radiation source

Text S4 Use of buffers in presence of humic acids

Text S5 Determination of $\text{SO}_4^{\bullet-}$ and $\bullet\text{OH}$ rate constants with dissolved organic matter

Text S6 Determination of response factors of atra-imine in HPLC-DAD measurements

Figure S1 Degradation of pCBA vs. atrazine during thermal activation of $\text{S}_2\text{O}_8^{2-}$ at 40 °C, 50 °C and 60 °C

Figure S2 Chromatogram of atrazine degradation by $\text{SO}_4^{\bullet-}$ generated in thermal activation of $\text{S}_2\text{O}_8^{2-}$

Figure S3 a) Calibration of atra-imine; b) hydrolysis of atra-imine

Figure S4 Spectra of atrazine, atra-imine and DIA

Text S1 Competition kinetics

Principle

Second order reaction rate constants of sulfate radicals ($\text{SO}_4^{\bullet-}$) were determined by competition kinetics in analogy to Peter and von Gunten [1]. Thereby, the observed degradation rate of a probe compound under study (P) is related to the observed degradation rate of a reference compound (R) (note that both compounds have to experience the same exposure of the oxidant, e.g., by their simultaneous degradation in one reaction system). The second order rate constant of a probe compound P can be derived from Equation S1

$$\ln\left(\frac{P}{P_0}\right) = \ln\left(\frac{R}{R_0}\right) \cdot \frac{k(P + \text{SO}_4^{\bullet-})}{k(R + \text{SO}_4^{\bullet-})}$$

by plotting $\ln\left(\frac{P}{P_0}\right)$ against the degradation of a reference compound $\ln\left(\frac{R}{R_0}\right)$, revealing a linear function (cf. Figure S1). The reaction rate of the probe compound can be calculated from the slope of this function multiplied by the reaction rate of the competitor. 5 μM of both, the competitor and the probe compound were added in the present study. Further detailed information about competition kinetics is provided by von Sonntag and von Gunten [2].

Competition kinetics at elevated temperatures

$\text{SO}_4^{\bullet-}$ were generated by thermolysis of $\text{S}_2\text{O}_8^{2-}$ at 60°C. It is important to point out that the reaction rate determined by competition kinetics (see above) under such condition corresponds to the temperature at which the reaction rate of the competitor has been determined (typically 20-25°C). This is due to the fact that the activation energies in the reaction with radicals such as $\text{SO}_4^{\bullet-}$ and $\bullet\text{OH}$ hardly differ between different reaction partners. This has been verified by conducting competition kinetics experiments with atrazine and 4-chlorobenzoic acid in presence of $\text{SO}_4^{\bullet-}$ generated by thermal activation of $\text{S}_2\text{O}_8^{2-}$ at

different temperatures. This couple of compounds (pCBA and atrazine) is suited well for this kind of test, since their reaction rates differ by nearly one order of magnitude, thus, representing a worst case scenario with regard to difference in activation energies. Figure S1 shows a double logarithmic plot of pCBA vs. atrazine according to Equation S1 during thermal activation of $\text{S}_2\text{O}_8^{2-}$ at 40, 50, and 60°C.

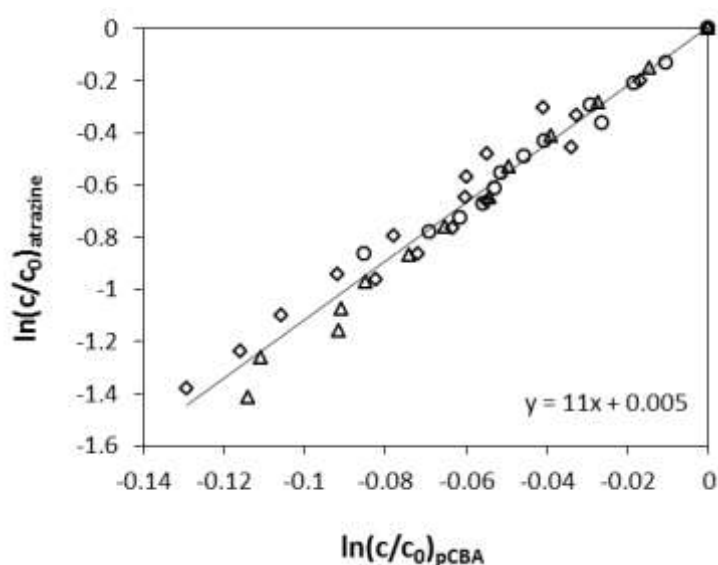


Figure S1: Degradation of pCBA vs. atrazine during thermal activation of $\text{S}_2\text{O}_8^{2-}$ at 40 °C (circles), 50 °C (triangles) and 60 °C (diamonds); $[\text{pCBA}]_0 = 4.71 \pm 0.02 \mu\text{M}$, $[\text{atrazine}]_0 = 4.63 \pm 0.12 \mu\text{M}$; $[\text{S}_2\text{O}_8^{2-}]_0 = 1 \text{ mM}$; initial pH: 7-8

It can be seen, that data obtained from thermal activation at all temperatures lie on one line indicating that differences in activation energy can be neglected. From this plot a reaction rate for atrazine of $4.0 \times 10^9 \text{ M}^{-1} \text{ s}^{-1}$ can be obtained which fairly well matches the value of Manoj determined by laser flash photolysis ($3 \times 10^9 \text{ M}^{-1} \text{ s}^{-1}$ [3]).

Text S2 Calculation of fractions reacting with an oxidant

The fraction of an oxidant (or other reactive species) reacting with a certain compound in competition with other solutes can be calculated if the corresponding concentrations and

reaction rate constants are known. The fraction corresponds to the concentration times the rate constant of the compound under study, divided by the sum of concentration times rate constants of all compounds reacting with the oxidant. Equation 2 gives an example for the fraction of hydroxyl radicals ($\bullet\text{OH}$) reacting with atrazine ($f(\text{atrazine})$) in presence of para-chlorobenzoic acid (pCBA) ($[\text{atrazine}]$ and $[\text{pCBA}]$ = concentration of atrazine and pCBA in M, $k(\bullet\text{OH} + \text{atrazine})$, $k(\bullet\text{OH} + \text{pCBA})$ = second order reaction rate constant of the reaction of $\bullet\text{OH}$ with atrazine and pCBA, respectively in $\text{M}^{-1} \text{s}^{-1}$).

$$\text{Equation S2} \quad f(\text{atrazine}) = \frac{[\text{atrazine}] \times k(\bullet\text{OH} + \text{atrazine})}{[\text{atrazine}] \times k(\bullet\text{OH} + \text{atrazine}) + [\text{pCBA}] \times k(\bullet\text{OH} + \text{pCBA})}$$

Text S3 Radiation source

For photochemical experiments a merry-go-round apparatus has been purchased from Hans und Thomas Schneider Glasapparatebau in Kreuzwertheim. This apparatus was equipped with a low pressure mercury arc from Heraeus Noble Light (GPH303T5L/4, 15 W). This radiation source emits nearly monochromatic light at 254 nm. The quartz glass of this radiation source is not transparent for the minor emission at 185 nm. A water filter with an optical path length of ca. 1 cm served as an additional safeguard. Thus, effects by 185 nm radiation can be neglected.

Text S4 Use of buffers in presence of humic acids

For preventing speciation of the humic acids, which could cause changes in the reactivity towards $\text{SO}_4^{\bullet-}$ and $\bullet\text{OH}$, buffering of pH was necessary (pH = 7.2). Therefore 1.25-2.5 mM phosphate was added. Due to the high concentration of humic acids (7.5-15 mgC L^{-1}) only a minor fraction of $\text{SO}_4^{\bullet-}$ is expected to react with the phosphate species and interferences by phosphate radicals can be neglected as will be explained below. The second order reaction rate constants of $\text{SO}_4^{\bullet-}$ with phosphate species are small ($k(\text{HPO}_4^{2-} + \text{SO}_4^{\bullet-}) = 1.2 \times 10^6 \text{ M}^{-1}$

s⁻¹ [4] $k(\text{H}_2\text{PO}_4^- + \text{SO}_4^{\bullet-}) \leq 7.4 \times 10^4 \text{ M}^{-1} \text{ s}^{-1}$ [5]). Due to the high DOC concentration, the reaction rate of $\text{SO}_4^{\bullet-}$ plus DOC has to be below $1000 \text{ L mg}^{-1} \text{ C s}^{-1}$ for enabling a > 10% fraction of $\text{SO}_4^{\bullet-}$ reacting with phosphate (calculations done using the principle explained in Text S2). Yet, for the $\text{SO}_4^{\bullet-}$ being similar reactive as $\bullet\text{OH}$ a reaction rate < $1000 \text{ L mg}^{-1} \text{ C s}^{-1}$ is unlikely (average reaction rate $k(\bullet\text{OH} + \text{DOC}) = 2.5 \times 10^4 \text{ L mg}^{-1} \text{ C s}^{-1}$ [6, 7], note that a reaction rate of the reaction $\text{SO}_4^{\bullet-}$ with humic acids was determined in the present study to be $6.8 \pm 0.3 \times 10^3 \text{ L mgC}^{-1} \text{ s}^{-1}$). Hence, the above assumption is justified.

Text S5 Determination of $\text{SO}_4^{\bullet-}$ and $\bullet\text{OH}$ rate constants with dissolved organic matter

The reaction rate constants of DOC plus $\text{SO}_4^{\bullet-}$ and $\bullet\text{OH}$ have been determined as will be described in the following. It has to be mentioned, that the photochemical calculations below are in analogy to Katsoyiannis et al. [8].

In the present system $\text{SO}_4^{\bullet-}$ and $\bullet\text{OH}$ are mainly scavenged by DOC competing for the degradation of atrazine. Since $k(\text{SO}_4^{\bullet-})$ and $k(\bullet\text{OH})$ of atrazine are known, the reaction rates of $\bullet\text{OH}$ and $\text{SO}_4^{\bullet-}$ plus DOC can be calculated on basis of the fluence rate and first order degradation of atrazine. The corresponding relationship is shown in Equation S3.

Equation S3

$$k' = \frac{2.303 \times \varepsilon_{\text{peroxide}} \times \phi_{\text{peroxide}} \times H \times [\text{peroxide}] \times k(\text{atrazine} + \text{radical})}{[\text{DOC}] \times k(\text{DOC} + \text{radical})} + k(\text{photolysis of atrazine})$$

$k'(\text{atrazine})$: First order degradation rate of atrazine / s^{-1}

$\varepsilon_{\text{peroxide}}$: Molar absorption coefficient of H_2O_2 or $\text{S}_2\text{O}_8^{2-}$ / $\text{m}^2 \text{mol}^{-1}$

ϕ_{peroxide} : Quantum yield of H_2O_2 or $\text{S}_2\text{O}_8^{2-}$ / mol Einstein^{-1}

H : Fluence rate / $\text{Einstein m}^{-2} \text{s}^{-1}$

$[\text{peroxide}]$: Concentration of H_2O_2 or $\text{S}_2\text{O}_8^{2-}$ / M

$k(\text{atrazine} + \text{radical})$: Second order rate constant of atrazine plus $\bullet\text{OH}$ or $\text{SO}_4^{\bullet-}$ / $\text{M}^{-1} \text{s}^{-1}$

$k(\text{photolysis of atrazine})$: Rate of atrazine photolysis / s^{-1}

$[\text{DOC}]$: Concentration of DOC / mgC L^{-1}

$k(\text{DOC} + \text{radical})$: Rate constant of the reaction $\bullet\text{OH}$ or $\text{SO}_4^{\bullet-}$ plus DOC / $\text{LmgC}^{-1} \text{s}^{-1}$

As the only unknown, $k(\text{DOC} + \text{radical})$ can either be derived by calculating the first order degradation rate of atrazine (experimental data) and solving the above Equation 3 for $k(\text{DOC} + \text{radical})$, or by adjusting $k(\text{DOC} + \text{radical})$ arriving at the best fit for the experimentally determined degradation of atrazine. The latter method has been used in the present study for different DOC and peroxide concentrations.

Following reaction parameters have been applied:

- quantum yield of H_2O_2 (254 nm, radical formation) : $1 \text{ mol Einstein}^{-1}$ [9]
- quantum yield of $\text{S}_2\text{O}_8^{2-}$ (254 & 248 nm, radical formation) : $1.4 \text{ mol Einstein}^{-1}$ [10, 11]
- molar absorption of H_2O_2 at 254 nm : $1.86 \text{ m}^2 \text{mol}^{-1}$ [8]
- molar absorption of $\text{S}_2\text{O}_8^{2-}$ at 254 nm : $2.2 \text{ m}^2 \text{mol}^{-1}$ [12]
- second order rate constant of atrazine plus $\text{SO}_4^{\bullet-}$ and $\bullet\text{OH}$: $3 \times 10^9 \text{ M}^{-1} \text{s}^{-1}$

153 The small fraction of radicals scavenged by the phosphate buffer (H_2PO_4^- and HPO_4^{2-}) and
 154 by the corresponding peroxide (H_2O_2 or $\text{S}_2\text{O}_8^{2-}$) was also considered. Therefore the following
 155 terms have to be included in the denominator in Equation S3:

$$156 \quad [\text{H}_2\text{PO}_4^-] \times k(\text{H}_2\text{PO}_4^- + \text{radical}) + [\text{HPO}_4^{2-}] \times k(\text{HPO}_4^{2-} + \text{radical}) + [\text{peroxide}] \times k(\text{peroxide} \\ 157 \quad + \text{radical})$$

158 With:

159 $[\text{H}_2\text{PO}_4^-]$: Concentration of dihydrogen phosphate / M

160 $[\text{HPO}_4^{2-}]$: Concentration of hydrogen phosphate / M

161 $[\text{peroxide}]$: Concentration of corresponding peroxide (H_2O_2 or $\text{S}_2\text{O}_8^{2-}$) / M

162 $k(\text{H}_2\text{PO}_4^- + \text{radical})$: Second order reaction rate constant of H_2PO_4^- plus $\bullet\text{OH}$ or $\text{SO}_4^{\bullet-}$ / M^{-1}
 163 s^{-1}

164 $k(\text{HPO}_4^{2-} + \text{radical})$: Second order reaction rate constant of HPO_4^{2-} plus $\bullet\text{OH}$ or $\text{SO}_4^{\bullet-}$ / M^{-1}
 165 s^{-1}

166 $k(\text{peroxide} + \text{radical})$: Second order reaction rate constant of corresponding peroxide (H_2O_2
 167 or $\text{S}_2\text{O}_8^{2-}$) plus $\bullet\text{OH}$ or $\text{SO}_4^{\bullet-}$ / $\text{M}^{-1} \text{ s}^{-1}$

168

169 The concentrations of the phosphate species result from the total phosphate buffer
 170 concentration and the corresponding pH (i.e., pH 7.2)

171 The corresponding rate constants for the phosphate species can be obtained from
 172 Maruthamuthu and Neta [5]. The reaction rates for the reaction of $\bullet\text{OH}$ with H_2O_2 can be
 173 obtained from Buxton et al.,[13] and the reaction rate of the reaction of $\text{SO}_4^{\bullet-}$ with $\text{S}_2\text{O}_8^{2-}$
 174 can be found in Herrmann et al.,[14].

175

176

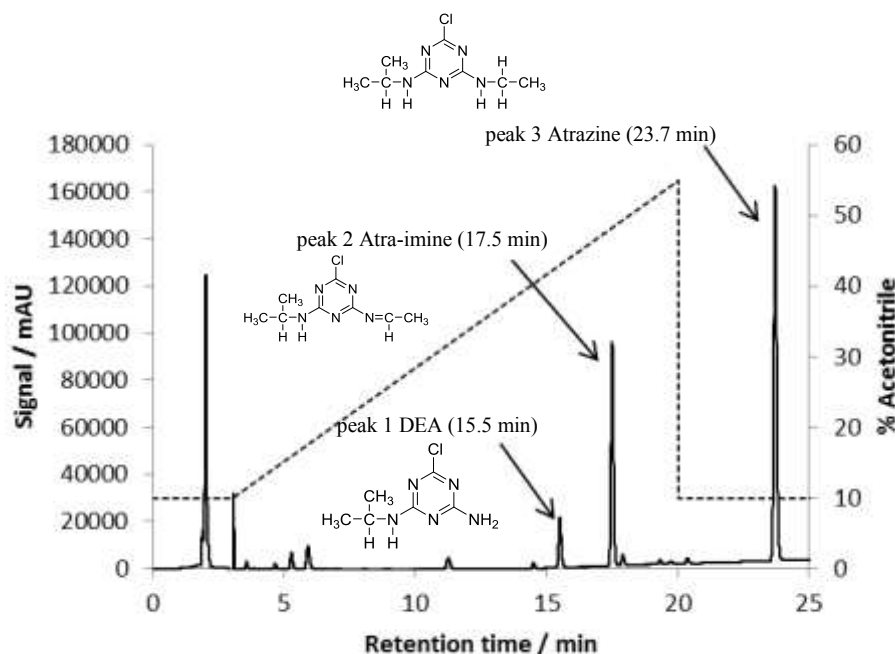


Figure S2 Chromatogram of atrazine degradation by $\text{SO}_4^{\bullet-}$ generated in thermal activation of $\text{S}_2\text{O}_8^{2-}$ (60°C , $[\text{atrazine}]_0 = 21 \mu\text{M}$, $[\text{S}_2\text{O}_8^{2-}]_0 = 1 \text{ mM}$, reaction time = 8 min, initial pH = 7; eluent acetonitrile/water (pH6-7)); DEA: Desethylatrazine, chemical structures are shown in the figure.

Text S6 Determination of response factors of atra-imine in HPLC-DAD measurements

Atra-imine was calibrated in an experiment whereupon hydrolysis of atra-imine DEA formation was monitored over time (half-life time of atra-imine was $\approx 7 \text{ h}$ (Figure S3)). Atra-imine was formed at experimental conditions given in the caption of Figure S2. Assuming a 100% yield of DEA arising from hydrolysis of atra-imine, the DEA formation corresponds to the amount of the hydrolyzed atra-imine. Thus, a plot of the atra-imine peak area vs. concentration of formed DEA, yields the required response factor of atra-imine ($\approx 99000 \text{ mAU} \times \text{min} \mu\text{M}^{-1}$ (213 nm)) (Figure S3). This response is very similar compared to DEA ($\approx 91000 \text{ mAU} \times \text{min} \mu\text{M}^{-1}$, 213 nm). Furthermore, the UV-spectra of atrazine, atra-imine and DEA obtained from the DAD hardly differ (Figure S4). Thus, calibration of DEA fairly works for atra-imine in the spectral range where DEA gives a fair response (i.e., 210 and 240 nm).

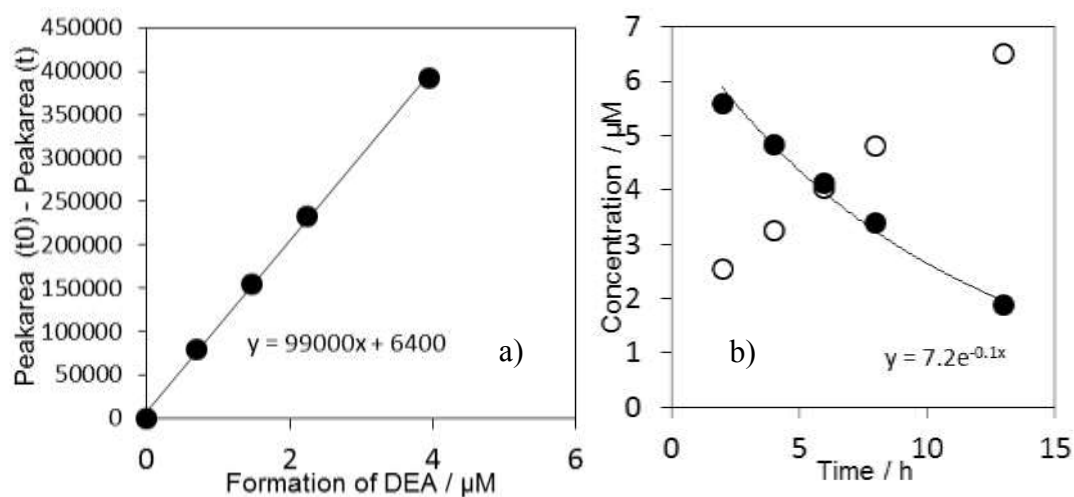


Figure S3 a) Calibration of atra-imine; b) hydrolysis of atra-imine: closed symbols atra-imine, open symbols DEA; $\text{pH} \approx 7$, $T = 20\text{-}25^\circ\text{C}$

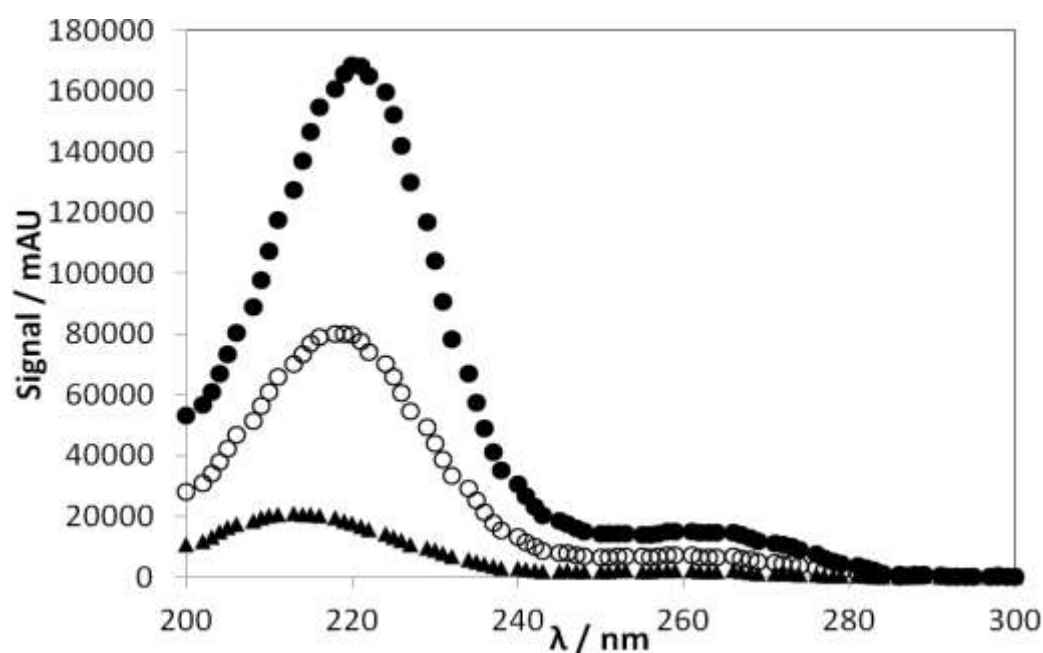


Figure S4: Spectra of atrazine (closed circles), Schiff base (N-ethyl side chain) (open circles) and DEA (triangles) obtained from the HPLC-DAD-measurement.

206 Literature

- 207 1. Peter, A.; von Gunten, U., Oxidation kinetics of selected taste and odor compounds
208 during ozonation of drinking water. *Environ. Sci. Technol.*, **2007**. 41(2): 626-631.
- 209 2. von Sonntag, C.; von Gunten, U., eds. *Chemistry of ozone in water and wastewater*
210 *treatment*. 2012, IWA Publishing.
- 211 3. Manoj, P.; Prasanthkumar, K.P.; Manoj, V.M.; Aravind, U.K.; Manojkumar, T.K.;
212 Aravindakumar, C.T., Oxidation of substituted triazines by sulfate radical anion
213 ($\text{SO}_4^{\bullet-}$) in aqueous medium: A laser flash photolysis and steady state radiolysis study.
214 *J. Phys. Org. Chem.*, **2007**. 20(2): 122-129.
- 215 4. Neta, P.; Huie, R.E.; Ross, A.B., Rate constants for reactions of inorganic radicals in
216 aqueous solution. *J. Phys. Chem. Ref. Data*, **1988**. 17(3): 1027 - 1040.
- 217 5. Maruthamuthu, P.; Neta, P., Phosphate radicals. Spectra, acid-base equilibria, and
218 reactions with inorganic compounds. *J. Phys. Chem.*, **1978**. 82(6): 710-713.
- 219 6. Schwarzenbach, R.P.; Gschwend, P.M.; Imboden, D.M., eds. *Environmental organic*
220 *chemistry*. John Wiley & Sons, Inc. ISBN 0-47 1-35750-2. 2003.
- 221 7. von Sonntag, C., Advanced oxidation processes: Mechanistic aspects. *Water Sci.*
222 *Technol.*, **2008**. 58: 1015-1021.
- 223 8. Katsoyiannis, I.A.; Canonica, S.; von Gunten, U., Efficiency and energy requirements
224 for the transformation of organic micropollutants by ozone, $\text{O}_3/\text{H}_2\text{O}_2$ and $\text{UV}/\text{H}_2\text{O}_2$.
225 *Water Res.*, **2011**. 45(13): 3811-3822.
- 226 9. Legrini, O.; Oliveros, E.; Braun, A.M., Photochemical processes for water treatment.
227 *Chem. Rev.*, **1993**. 93(2): 671-698.
- 228 10. Herrmann, H., On the photolysis of simple anions and neutral molecules as sources of
229 O^-/OH , SO_x^- and Cl in aqueous solution. *Phys. Chem. Chem. Phys.*, **2007**. 9(30):
230 3935-3964.
- 231 11. Mark, G.; Schuchmann, M.N.; Schuchmann, H.P.; von Sonntag, C., The photolysis of
232 potassium peroxodisulphate in aqueous solution in the presence of tert-butanol: a
233 simple actinometer for 254 nm radiation. *J. Photochem. Photobiol., A*, **1990**. 55(2):
234 157-168.
- 235 12. Heidt, L.J., The photolysis of persulfate. *J. Chem. Phys.*, **1942**. 10(5): 297-302.
- 236 13. Buxton, G.V.; Greenstock, C.L.; Helman, W.P.; Ross, A.B., Critical review of rate
237 constants for reactions of hydrated electrons, hydrogen-atoms and hydroxyl radicals
238 ($\text{OH}/\text{O}^\bullet$) in aqueous solution. *J. Phys. Chem. Ref. Data*, **1988**. 17(2): 513-886.
- 239 14. Herrmann, H.; Reese, A.; Zellner, R., Time-resolved UV/VIS diode array radical
240 anions in aqueous solution absorption spectroscopy of SO_x^- ($x=3, 4, 5$). *J. Mol.*
241 *Struct.*, **1995**. 348: 183-186.